Stem cell receptor degradation by niche cells restricts signalling

Sophia Ladyzhets[1] and Mayu Inaba[1, *]

1. Department of Cell Biology, University of Connecticut Health Center, Farmington, CT 06030

[*] Correspondence: inaba@uchc.edu

Abstract:

The stem cell niche utilizes short-range signalling, such that only stem cells but not their differentiating progeny receive self-renewing signals[1]. A cellular projection, the microtubule-based nanotube (MT-nanotube), projects from *Drosophila* male germline stem cells (GSCs) into niche "hub" cells, ensuring that GSC-produced receptor Thickveins (Tkv) receives sufficient hub-produced ligand Decapentaplegic (Dpp) while excluding non-stem cells from self-renewing signal activation. Here we show that GSC-produced Tkv is taken up by hub cells from the MT-nanotube and degraded in lysosomes. Failure of the hub cells to take up Tkv, or perturbation of hub cell lysosomal function lead to excess Tkv within GSCs, elevated downstream signal activation, and GSC tumor formation in non-niche locations. We propose that down-regulation of the self-renewal factor receptor by niche cells restricts the ligand/receptor interaction to the surface of the MT-nanotube membrane, fine-tuning the span of the short-range niche-stem cell signalling, and that this may be a general feature of contact-dependent signalling.

The stem cell niche is the regulatory microenvironment in which stem cells reside. The niche sends signals to stem cells to maintain stem cell identity. At the *Drosophila* testes apical tip, 8 to 10 GSCs surround the hub, the cluster of niche cells (Figure 1A, left). Hub cells produce Unpaired (Upd) and Dpp ligands, both of which are required for GSC maintenance [2 3]. GSCs divide with their mitotic spindle oriented perpendicular to the hub-GSC interface (mitotic GSC in Figure 1A, left). Consequently, one daughter cell attached to the hub remains a stem cell, while the other daughter displaced away from the hub differentiates into a gonialblast (GB) [2 4] (Figure 1A, left, a red arrow

indicates division orientation). Ectopic expression of the niche ligands leads to tumorous proliferation of undifferentiated germ cells outside the niche [2 5 6 7 8 9]. Therefore, the range of the signal must be tightly regulated to activate signalling only within the cells that are juxtaposed to the hub, without erroneously activating the signal in differentiating cells. However, our understanding of the mechanisms that defines the range of the niche remains limited.

Previously, we demonstrated that MT-nanotubes form specifically at the hub-GSC interface and protrude from GSCs into hub cells. The niche ligand, Dpp, and its receptor, Tkv, interact at the nanotube-hub membrane contact sites, resulting in efficient and specific signal activation [10] (Figure 1A, right). We reported that a fully functional Tkv -GFP protein expressed in germline cells localizes to the MT-nanotubes, as they are trafficked along the MT-nanotubes. Thus, we observe the Tkv-GFP only at the hub area and Tkv-GFP signal is barely seen in the cell body of GSC (Figure S1A). However, suppression of MT-nanotube formation by knockdown of *intraflagellar transport (IFT)-B* (*osm6*, and *oseg2*) lead to retention of Tkv on the GSC plasma membrane [10] (Figure S1B-C recapitulates the data shown in previous publication). In addition to the localization of Tkv to the MT-nanotube membrane, we have noted Tkv-GFP 'puncta' within the hub cells outside of the MT-nanotubes (Figure S1A) [10]. The Tkv-GFP punctae in the hub often colocalize with lysosomes (Figure 1B and D), leading us to hypothesize that Tkv-GFP protein is degraded in hub lysosomes. Similar punctae were observed in Tkv protein trap line (functionally validated exon trap insertion of Venus[11], Figure 1C) also colocalizing with lysotracker within hub cells (Figure 1E). By inducing GSC clones that co-express Tkv–mCherry and GFP–αTub, similar puncta were observed in the hub, but only in the vincinity of the clone, indicating that the Tkv observed within lysosomes expressed in the GSC clone (Figure 1F). To confirm the lysosomal localization of Tkv, we suppressed lysosomal-dependent degradation using chloroquine, a drug that raises lysosomal pH and inhibits lysosomal enzymes. Treatment of isolated testes with chloroquine significantly increased the size of Tkv-GFP punctae within the hub (Figure 1G, H, and I). Abnormal distribution of Tkv-GFP on the GSC plasma membrane was also often observed (Figure 1J, arrows), confirming that Tkv-GFP is degraded in hub lysosomes. Same trends were observed by using Tkv-trap line (Figure 1K, L and M). These data suggest that lysosome-mediated degradation of Tkv within the hub contributes to downregulation of Tkv in the GSC, thus preventing Tkv localization outside the MT-nanotubes. Small fraction of Tkv-GFP punctae also seen in GSCs with or without chloroquine treatment were much less prominent within GSCs and their immediate progenies compared with the hub (Figure 1G, H, J, K, L, yellow arrowheads). It has to be noted that Chloroquine treatment clearly increased the Tkv-trap signal in

the lysosome and plasma membrane of later stage spermatogonia (Figure 1L distal from yellow broken line, and L' yellow arrowheads), indicating that spermatogonia likely utilize their own lysosomes to degrade Tkv.

A similar co-localization with lysosomes was also observed for Dpp ligand punctae (Figure S2A), indicating that the Tkv-GFP downregulation could occur after engaging with the Dpp ligand. We could not uncover whether lysosomal degradation requires the prior interaction with Dpp ligand or not. Domeless-GFP, the receptor for another ligand Upd, did not localize to lysosomes in the hub; this lack of localization indicates the selectivity of this regulation (Figure S2B).

To examine whether defective lysosomal degradation alters the signalling strength of the Dpp-Tkv pathway, we measured the level of phosphorylated Mad (pMad) in GSCs, a downstream target [10]. Genes involved in lysosomal-dependent degradation were knocked down using GAL4-UAS system. Hub- (and/or germ cell-) specific promoter-driven GAL4 drivers were used to determine the cell type in which these genes are functioning (Figure 2A-D control). Spinster (Spin) is a putative lysosomal H^+-carbohydrate transporter and a common regulator of lysosomal biogenesis, as well as a known regulator of Dpp signalling [12 13]. Lysosomal-associated membrane protein 1 (Lamp1) is an abundant protein in the lysosomal membrane and is required for lysosomes to fuse with endosomes/autophagosomes [14]. Germ cell-specific knockdown of these lysosomal genes did not alter pMad level (Figure 2E, G, and M). In contrast, hub-specific downregulation of these genes led to a significant increase in pMad level, indicating that lysosomal activity in the hub cells is required to dampen Dpp signalling (Figure 2F, H, and M).

We tested the effect of knockdown of genes required for membrane vesicle trafficking, which is potentially utilized for Tkv-containing vesicle formation and sorting. We found that these genes are required to regulate pMad level in GSCs but not in the hub cells (Figure 2I-L, M). Deep Orange (Dor), the *Drosophila* homolog of Vps18 (Vacuolar protein sorting-associated protein 18), acts as a core component of the endosomal tethering complexes proposed to be involved in the early-to-late endosome conversion [15]. Knockdown of *dor* in germ cells (but not in hub cells) increased pMad level in GSCs (Figure 2I, J and M). The endosomal sorting complexes required for transport (ESCRT) assemble into a multi-subunit machine that performs membrane bending and scission. Specifically, ESCRT-III can facilitate the outward budding such as virus budding [16], Similar machinery might be utilized on the GSC side of the GSC-Hub interaction, where Tkv-containing membrane budding may occur in the "outward" direction, from the GSC to the hub cell. Indeed, knockdown of *Shrub* (*shrb*) gene (a subunit of the ESCRT-III complex [17 18]) in GSCs (but not in hub cells) increased pMad level

in GSCs. (Figure 2K, L and M). *dpp* mRNA levels showed no detectible alteration in lysosomal defective hub cells (Figure S3 A and B), indicating that regulation of the *dpp* signal by hub cell lysosomes is not caused by a change in niche ligand production.

SMAD ubiquitination regulatory factor (Smurf)-mediated Tkv ubiquitination is necessary for GSC differentiation both in testicular and ovarian GSCs [3 19]. Smurf is a HECT (Homologous to the E6-AP Carboxyl Terminus) domain protein with E3 ubiquitin ligase activity, and disruption of Smurf function enhances Dpp-Tkv signal activation [19]. Ubiquitination of membrane proteins is required for recognition by ESCRT, and thus is required for endocytosis, lysosomal fusion, and degradation [20]. To determine if ubiquitination-defective Tkv no longer localizes to hub cells we generated a UAS-*tkv*-S238A-GFP transgenic line that carries a phosphorylation site mutation required for Smurf-mediated ubiquitination [3]. Tkv-S238A-GFP protein was not detected in hub cell lysosomes and exhibited strong retention withixn GSCs compared to wildtype Tkv-GFP protein (Figure 3A, B), indicating that Tkv-S238A protein is not transferred from GSCs to hub cells. A small fraction of Tkv-GFP foci were still observed in the hub area, often contacting lysosomes (Figure 3B', D, E) but not precisely colocalized (Figure 3C, E), suggesting that the fusion step of receptor-containing vesicles with lysosomes is also impaired. Moreover, expression of Tkv-S238A-GFP in GSC resulted in elevated signal activation as indicated by higher pMad levels (Figure 3F, G, H). Thus, Tkv protein is the target of lysosomal degradation in hub cells, allowing hub lysosomes to negatively regulate Dpp signalling.

We wanted to understand the consequence of failure to traffic Tkv to the MT-nanotubes. We previously demonstrated that the MT-nanotube is required for signal reception, thus interfering with MT-nanotube-formation by knockdown of *IFT-B* (*oseg2*, *osm6*, and *che-13*) reduced pMad levels in GSCs [10]. Here we found that knockdown of *IFT-B* frequently caused GSC tumors in non-niche locations where Tkv-GFP is also expressed (Figure 4A-C). Under these conditions, the over-expressed Tkv localized to the GSC plasma membrane, likely because GSCs were unable to process Tkv via nanotube transport for hub-mediated degradation. The GSC-like tumour phenotype was caused by a defect within GSCs and their immediate progeny rather than a defect in later stage spermatogonia, since use of the bamGal4 driver (active in 4- to 8-cell stage spermatogonia), instead of the nosGal4 driver, to mediate *IFT-B* knockdown, and Tkv-GFP overexpression, did not cause tumour formation (Figure 4C, Figure S4). These data strongly suggest that receptor protein degradation within niche cell lysosomes contributes to restriction of niche size by inhibiting stem cell proliferation outside of the niche.

Most signalling pathways consist of many components, whose activity must be closely coordinated. Here we provide evidence that signal activation and inhibition occur via the same structure: MT-nanotubes. MT-nanotubes transport Tkv receptors into the hub to interact with the Dpp ligand pool, promoting signal reception. They also guide Tkv receptor transport from the GSC membrane to niche (hub) cell lysosomes for destruction (Figure S5). Lysosomal localization-defective Tkv, and MT-nanotube loss, both cause Tkv retention along the entire GSC cortex, suggesting that the Tkv degradation limits the location for ligand/receptor interaction to the MT-nanotube membrane, rather than the entire GSC membrane, preventing the receptor from entering differentiating daughter cells during cell division.

Our study demonstrates that lysosomal degradation of a receptor can occur in neighbouring cells, rather than the receptor-producing cell. Components mediating lysosomal function (Lamp1 and Spin) are required in neighbouring hub cells (Figure S5). In contrast, components mediating vesicle trafficking (ESCRTIII and VPS-C) are required in GSC itself. MT-nanotube may shed its membrane directly into hub cells, the process being initiated by outward budding rather than inward budding of the plasma membrane (Figure S5). Consistent with this model, enhancing the MT-nanotube formation by knocking down *klp10A*, or overexpressing αTubulin, in GSCs substantially increased the appearance of double-membrane vesicles in hub cells (Figure 5A, 5B, and 5C), with 3D reconstitution indicating that these vesicles are not part of the MT-nanotubes, and instead were likely shed from MT-nanotubes. If GSCs endocytosed the receptor the cytoplasmic domain of Tkv would be facing the outside of endosomes and the signal could be transduced until it was degraded by fusion with a lysosome [21]. In our model, such endocytosis would not occur in GSCs. In hub cells the cytoplasmic domain would be sequestered inside the vesicle. Stem cells could employ this mechanism to rapidly shut down the signal without taking the receptor back into its own cells. However, Tkv is ubiquitinated on its cytoplasmic domain [22], raising the question of how vesicle recognition by the lysosome occurs. Alternatively, GSCs may endocytose receptor to form a multivesicular body prior to GSC to hub transfer.

Our previous discovery of MT-nanotube-mediated signalling revealed that niche and stem cells interact in a contact-dependent manner, enabling highly specific cell-cell interactions. To ensure specificity, “contact-independent” signal activation should not occur. This study demonstrates that niche cells carry out stem cell receptor digestion to restrict receptor localization to MT-nanotubes, preventing “contact-independent” ligand-receptor interactions outside of the MT-nanotubes. Cytonemes, another type of actin-dependent signalling protrusion [23] [24], transfer ligand and receptor,

allowing the interaction to occur in a contact-dependent manner between the cells at a distance. Ligand-producing and receptor-producing cells both form cytonemes and both cells have been observed to take up signalling proteins: receptor into the ligand-producing cells and ligand into the receptor-producing cells [24], indicating the universality of such transfer in general contact-dependent signalling.

Acknowledgements

We thank the Glastonbury High School Advanced Research Mentorship program and Diane Pintavalle for providing support to Sophia Ladyzhets; Christopher Bonin for manuscript editing; Michael Buszczak, Yukiko Yamashita, the Bloomington Drosophila Stock Center and the Developmental Studies Hybridoma Bank for reagents; Laurinda Jaffe, Mark Terasaki, Yukiko Yamashita and Rachael Norris for comments and advice, and the Inaba laboratory members for discussion. This work was supported by an NIH grant 1R35GM128678-01 and startup funds from UConn Health (to M.I.).

Author Contributions

M.I. conceived the project, M.I. and S.L. designed experiments and executed experiments, analysed the data, and wrote and edited the manuscript.

Figure legends

Figure 1. Tkv receptor expressed in GSCs, localizes to hub cell lysosomes. A, left, Schematic of the *Drosophila* male GSC niche. GSCs are attached to the hub. The immediate daughters of GSCs, the gonialblasts (GBs) are displaced away from the hub then start differentiation. A mitotic GSC is shown carrying a spindle that is perpendicular to the hub-GSC interface, leading to division orientation (red arrow indicates the division orientation of the daughter cells). **Right,** MT-nanotube-mediated Dpp ligand-Tkv receptor interaction at the hub cell-GSC boundary. **B,** Tkv-GFP localizing in the hub lysosomes (nosGal4>UAS-*tkv*-GFP). **C,** Tkv-trap (venus) localizing in the hub lysosomes. **B, C,** Arrowheads indicate colocalization (yellow) of Tkv (green) and lysosomes (red). **D, E,** Magnified images of hub area of nos>tkv-GFP (**D-D”**) and Tkv-trap (**E-E”**). **F,** A GSC clone expressing Tkv-mCherry, GFP-αTub and GFP (hs-flp, nos-FRT-stop-FRT-Gal4, UAS-GFP, UAS-GFP-*αtub*, UAS-*tkv*-mCherry). Arrowheads indicate localization of Tkv-mCherry (red). **G-J,**

Representative images of the hub area surrounded by Tkv-GFP-expressing GSCs in 4-hour cultured testes without (**G**) or with (**H, J**) chloroquine (+CQ). Arrowheads in H indicate enlarged Tkv-GFP punctae within the hub. Arrows in **J** indicate GSCs with plasma membrane Tkv localization. (Note: When testes possess GSCs with strong membrane Tkv after CQ treatment, enlarged Tkv punctae were not typically prominent in the hub area for an unknown reason.) **I, M,** Measured diameters (largest diameter chosen from 0.5 μm interval z-stacks for each dot) of Tkv punctae in the hub in control incubation without CQ or with CQ are plotted in the box-and-whisker plot. The indicated numbers (n) of dots from two independent experiments were scored for each data point. The *P* value was calculated by a student t-test. **K, L,** Representative images of the hub area of Tkv-trap testis in 4-hour cultured testes without (**K**) or with (**L**) chloroquine (+CQ). **L",** Magnified image of square region of **L'**. Arrows in **L** indicate GSCs with plasma membrane Tkv localization. Yellow arrowheads indicate Tkv punctae within GSCs (**G H J K L**) or late spermatogonia (**L"**).
Dotted blue line indicates the hub. Scale bars, 10 μm.

Figure 2. Hub lysosomes are responsible for Dpp signal suppression. A-L, Representative images of pMad staining (red) in testes from flies of indicated genotypes. Germ-cell (nosGal4) or hub cell (updGal4) specific drivers were used. updGal4^{ts} was used for *lamp1* and *shrb*, as they are lethal with updGal4 specific RNAi (see methods). pMad signal in somatic cyst cells (arrowheads) were used as internal control (nosGal4 and updGal4 both are not active in these cells, see methods). Scale bars, 10 μm. Asterisk indicates the hub. White line divides GSCs attached to the hub and their immediate progenies. Red arrowheads indicate cells away from the hub which remain pMad positive. Vasa (green); germ cell marker. Note: nos>*dor* RNAi showed GSC differentiation defects and tumorous proliferation. upd^{ts}Gal4>*shrb* RNAi occasionally showed an incomplete germ cell and cyst cell loss phenotype. **M,** Quantitation of pMad intensity in the GSCs (relative to CC). Indicated numbers of GSCs from at least two independent experiments were scored for each data point. Data are means and standard deviations. P values (****P<0.0001) are shown. Adjusted *P* values were calculated by Dunnett's multiple comparisons.

Figure 3. Tkv ubiquitination is required for localization in hub cell lysosomes.
A, B, Representative images of the hub area with germline Tkv-GFP expression (A, nosGal4>*tkv*-GFP), Tkv-S238A-GFP expression (B, nosGal4>*tkv*S238A-GFP). B' with Lysotracker dye staining

(red), GFP (green). Magnified images of the square region from B' are shown in B". **C, D,** Three-dimensional rendering showing colocalization (arrows) of lysosomes with Tkv (C) or contact (no colocalization, arrowheads) of lysosomes with TkvS238A (D). **E,** % of GFP positive lysosomes within the hub were scored for Tkv-GFP or TkvS238A-GFP expressing testes. Indicated numbers of dots from more than 5 testes were scored for both data points. **F, G,** Representative images of pMad staining in the testes with Tkv-GFP expression (F) or TkvS238A-GFP expression (G); red arrowheads indicate the cells with strong pMad outside of the niche. 1B1 (red) staining indicates the fusome, the germline-specific ER-like structure. **H,** Quantitation of pMad intensity in the GSCs (relative to CC) of Tkv- or TkvS238A-expressing testes. The indicated numbers of GSCs from two independent experiments were scored for each data point. Data are means and standard deviations. Adjusted *P* values from Dunnett's multiple comparisons test are provided. Scale bars, 10 μm unless otherwise stated.

Figure 4. MT-nanotubes are required for Dpp signal suppression outside of the niche. A, B, Representative images of Tkv-GFP over-expressing testes without (A) or with (B) *osm6* RNAi. Germ cells does not retain over-expressed Tkv-GFP (A). Note: Tkv-GFP punctae in the hub (and seen in Figure 1B) are not visible at this magnification. With *osm6* RNAi, germ cells retain the Tkv-GFP within the cells (B) and form germline tumours (yellow dotted line) positive for Tkv-GFP. **C,** % of tumour cell cluster-positive testes in Tkv-GFP over-expressing testes with the indicated *IFT-B* gene knockdown. The indicated numbers of testes from three independent experiments were scored for each data point. Data are means and standard deviations. Adjusted *P* values from Dunnett's multiple comparisons test are provided. Scale bars, 10 μm. Asterisk indicates approximate hub location.

Figure 5 Enhanced MT-nanotube formation increases the number of membranous vesicles in hub cells.

A-C, Representative images of Serial Block Face Scanning Electron Microscopy. Pink indicates the hub areas of Wildtype (A), nos>*klp10A* RNAi (B) and nos>GFP-*αtub* (C) testis. Arrowheads indicate large, translucent membrane vesicles increased in *klp10A* knockdown. Cytoplasms of hub cells are filled up with similar vesicles in the testis with GFP-*αtub* overexpression. Scale bars, 10 μm.

References

1. Morrison, S. J. & Kimble, J. Asymmetric and symmetric stem-cell divisions in development and cancer. *Nature* **441,** 1068–1074 (2006).
2. Kawase, E., Wong, M. D., Ding, B. C. & Xie, T. Gbb/Bmp signaling is essential for maintaining germline stem cells and for repressing bam transcription in the Drosophila testis. *Development* **131,** 1365–75 (2004).
3. Xia, L. *et al.* The Fused/Smurf complex controls the fate of Drosophila germline stem cells by generating a gradient BMP response. *Cell* **143,** 978–90 (2010).
4. Yamashita, Y. M., Jones, D. L. & Fuller, M. T. Orientation of asymmetric stem cell division by the APC tumor suppressor and centrosome. *Science.* **301,** 1547–1550 (2003).
5. Shivdasani, A. A. & Ingham, P. W. Regulation of Stem Cell Maintenance and Transit Amplifying Cell Proliferation by TGF-β Signaling in Drosophila Spermatogenesis. *Curr. Biol.* **13,** 2065–2072 (2003).
6. Schulz, C. *et al.* A misexpression screen reveals effects of bag-of-marbles and TGF beta class signaling on the Drosophila male germ-line stem cell lineage. *Genetics* **167,** 707–23 (2004).
7. Chen, D. & McKearin, D. Dpp signaling silences bam transcription directly to establish asymmetric divisions of germline stem cells. *Curr. Biol.* **13,** 1786–91 (2003).
8. Kiger, A. A., Jones, D. L., Schulz, C., Rogers, M. B. & Fuller, M. T. Stem cell self-renewal specified by JAK-STAT activation in response to a support cell cue. *Science (80-.).* **294,** 2542–5 (2001).
9. Tulina, N. & Matunis, E. Control of stem cell self-renewal in Drosophila spermatogenesis by JAK-STAT signaling. *Science* **294,** 2546–9 (2001).
10. Inaba, M., Buszczak, M. & Yamashita, Y. M. Nanotubes mediate niche-stem-cell signalling in the Drosophila testis. *Nature* **523,** 329–32 (2015).
11. Yuva-Aydemir, Y., Bauke, A.-C. & Klämbt, C. Spinster controls Dpp signaling during glial migration in the Drosophila eye. *J. Neurosci.* **31,** 7005–15 (2011).
12. Sweeney, S. T. & Davis, G. W. Unrestricted synaptic growth in spinster-a late endosomal protein implicated in TGF-beta-mediated synaptic growth regulation. *Neuron* **36,** 403–16 (2002).
13. Yuva-Aydemir, Y., Bauke, A.-C. & Klambt, C. Spinster Controls Dpp Signaling during

Glial Migration in the Drosophila Eye. *J. Neurosci.* **31,** 7005–7015 (2011).

14. Eskelinen, E.-L. Roles of LAMP-1 and LAMP-2 in lysosome biogenesis and autophagy. *Mol. Aspects Med.* **27,** 495–502 (2006).
15. Kaksonen, M. & Roux, A. Mechanisms of clathrin-mediated endocytosis. *Nat. Rev. Mol. Cell Biol.* **19,** 313–326 (2018).
16. Alonso Y Adell, M., Migliano, S. M. & Teis, D. ESCRT-III and Vps4: a dynamic multipurpose tool for membrane budding and scission. *FEBS J.* **283,** 3288–3302 (2016).
17. Matias, N. R., Mathieu, J. & Huynh, J.-R. Abscission is regulated by the ESCRT-III protein shrub in Drosophila germline stem cells. *PLoS Genet.* **11,** e1004653 (2015).
18. Vaccari, T. *et al.* Comparative analysis of ESCRT-I, ESCRT-II and ESCRT-III function in Drosophila by efficient isolation of ESCRT mutants. *J. Cell Sci.* **122,** 2413–23 (2009).
19. Chang, Y.-J., Pi, H., Hsieh, C.-C. & Fuller, M. T. Smurf-mediated differential proteolysis generates dynamic BMP signaling in germline stem cells during Drosophila testis development. *Dev. Biol.* **383,** 106–20 (2013).
20. Piper, R. C. & Lehner, P. J. Endosomal transport via ubiquitination. *Trends Cell Biol.* **21,** 647–655 (2011).
21. Clement, C. A. *et al.* TGF-β signaling is associated with endocytosis at the pocket region of the primary cilium. *Cell Rep.* **3,** 1806–14 (2013).
22. Li, W. *et al.* Angelman Syndrome Protein Ube3a Regulates Synaptic Growth and Endocytosis by Inhibiting BMP Signaling in Drosophila. *PLOS Genet.* **12,** e1006062 (2016).
23. Ramírez-Weber, F. a & Kornberg, T. B. Cytonemes: cellular processes that project to the principal signaling center in Drosophila imaginal discs. *Cell* **97,** 599–607 (1999).
24. Kornberg, T. B. & Roy, S. Cytonemes as specialized signaling filopodia. *Development* **141,** 729–36 (2014).
25. Salzmann, V., Inaba, M., Cheng, J. & Yamashita, Y. M. Lineage tracing quantification reveals symmetric stem cell division in drosophila male germline stem cells. *Cell. Mol. Bioeng.* **6,** 441–448 (2013).
26. Van Doren, M., Williamson, A. L. & Lehmann, R. Regulation of zygotic gene expression in Drosophila primordial germ cells. *Curr Biol* **8,** 243–246 (1998).
27. Ghiglione, C. *et al.* The Drosophila cytokine receptor Domeless controls border cell

migration and epithelial polarization during oogenesis. *Development* **129,** 5437–47 (2002).

28. McGuire, S. E., Le, P. T., Osborn, A. J., Matsumoto, K. & Davis, R. L. Spatiotemporal Rescue of Memory Dysfunction in Drosophila. *Science.* **302,** 1765–1768 (2003).
29. Roy, S., Huang, H., Liu, S. & Kornberg, T. B. Cytoneme-mediated contact-dependent transport of the Drosophila decapentaplegic signaling protein. *Science* **343,** 1244624 (2014).
30. Inaba, M. & Yamashita, Y. M. *Evaluation of the asymmetric division of Drosophila male germline stem cells*. *Methods in Molecular Biology* **1463,** (2017).
31. Raj, A. & Tyagi, S. Detection of Individual Endogenous RNA Transcripts In Situ Using Multiple Singly Labeled Probes. in *Methods in enzymology* **472,** 365–386 (2010).

Figure 1

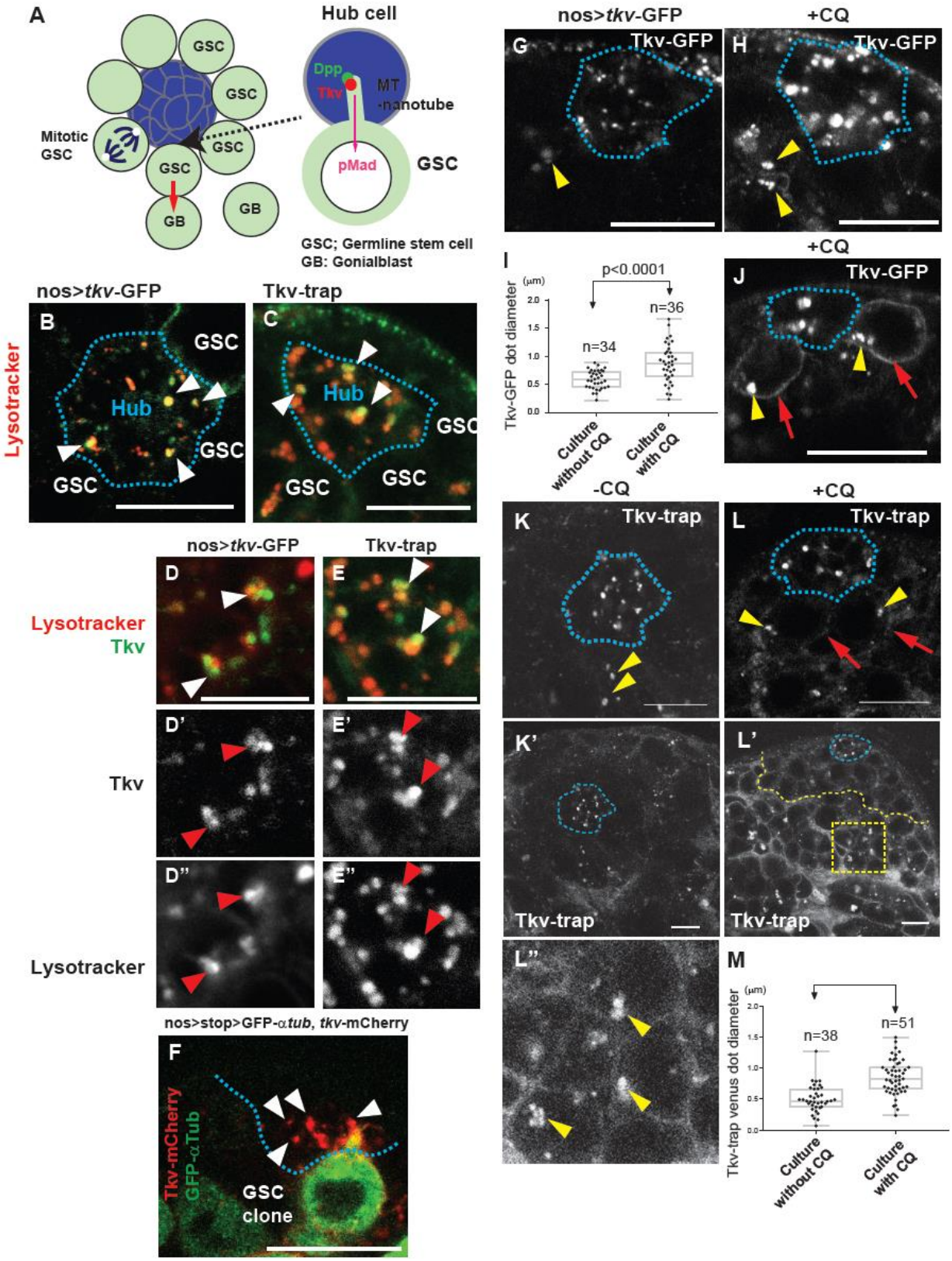
A
Hub cell
GSC
Mitotic GSC
GB
Dpp
Tkv
MT -nanotube
pMad
GSC; Germline stem cell
GB: Gonialblast
nos>tkv-GFP
Tkv-trap
Lysotracker
B
C
Hub
D
E
Lysotracker
Tkv
D'
E'
Tkv
D''
E''
Lysotracker
nos>stop>GFP-αtub, tkv-mCherry
F
Tkv-mCherry
GFP-αTub
GSC clone
G
H
Tkv-GFP
+CQ
I
p<0.0001
n=34
n=36
Tkv-GFP dot diameter
Culture without CQ
Culture with CQ
J
K
L
-CQ
Tkv-trap
K'
L'
L''
M
n=38
n=51
Tkv-trap venus dot diameter

Figure 2

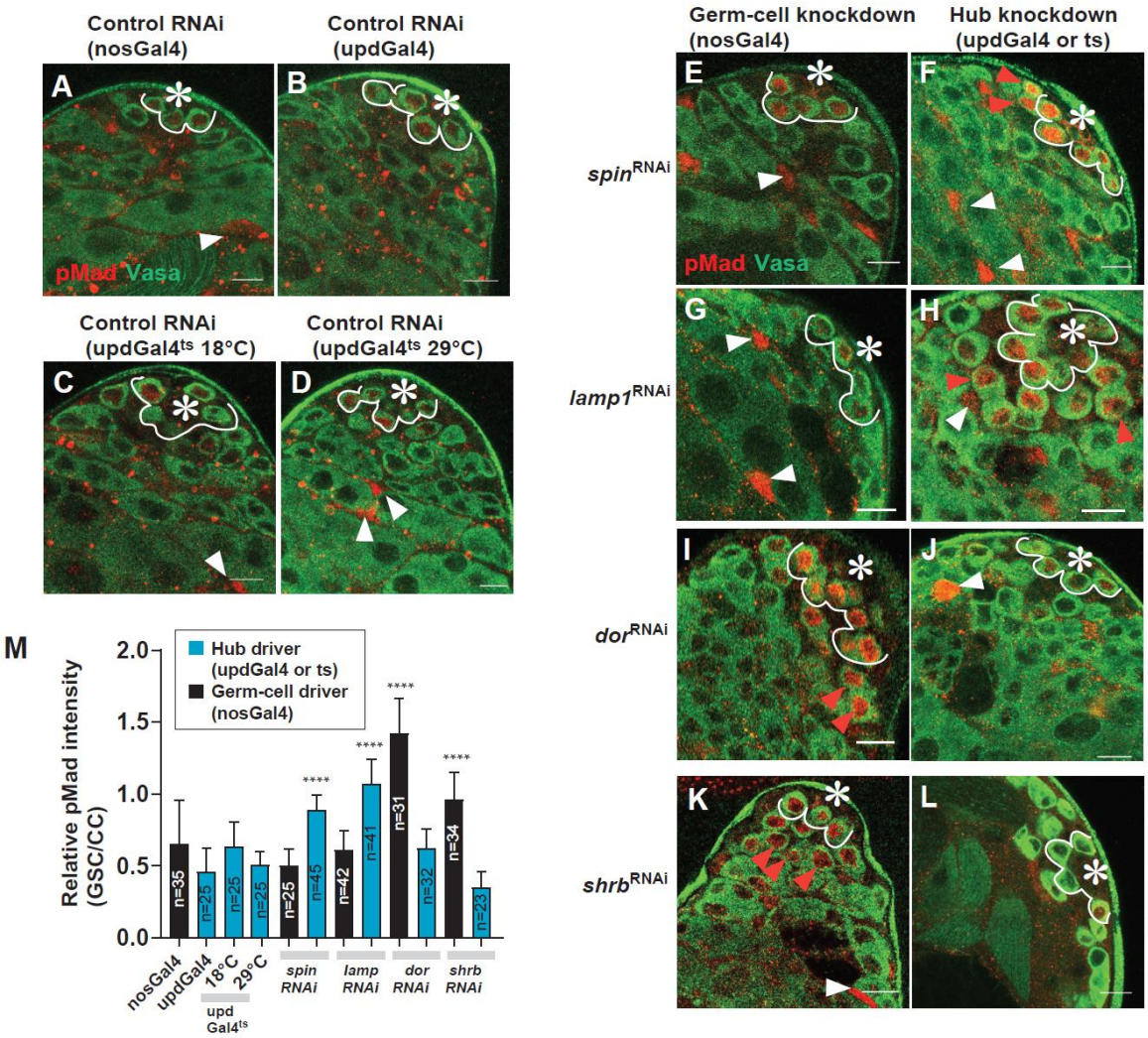
Control RNAi (nosGal4)
Control RNAi (updGal4)
Control RNAi (updGal4ts 18°C)
Control RNAi (updGal4ts 29°C)
A
B
C
D
pMad Vasa
Germ-cell knockdown (nosGal4)
Hub knockdown (updGal4 or ts)
E
F
G
H
I
J
K
L
spinRNAi
lamp1RNAi
dorRNAi
shrbRNAi
M
Relative pMad intensity (GSC/CC)
Hub driver (updGal4 or ts)
Germ-cell driver (nosGal4)
2.0
1.5
1.0
0.5
0.0
****
n=35
n=25
n=25
n=25
n=25
n=45
n=42
n=41
n=31
n=32
n=34
n=23
nosGal4
updGal4
18°C
29°C
upd Gal4ts
spin RNAi
lamp RNAi
dor RNAi
shrb RNAi

Figure 3

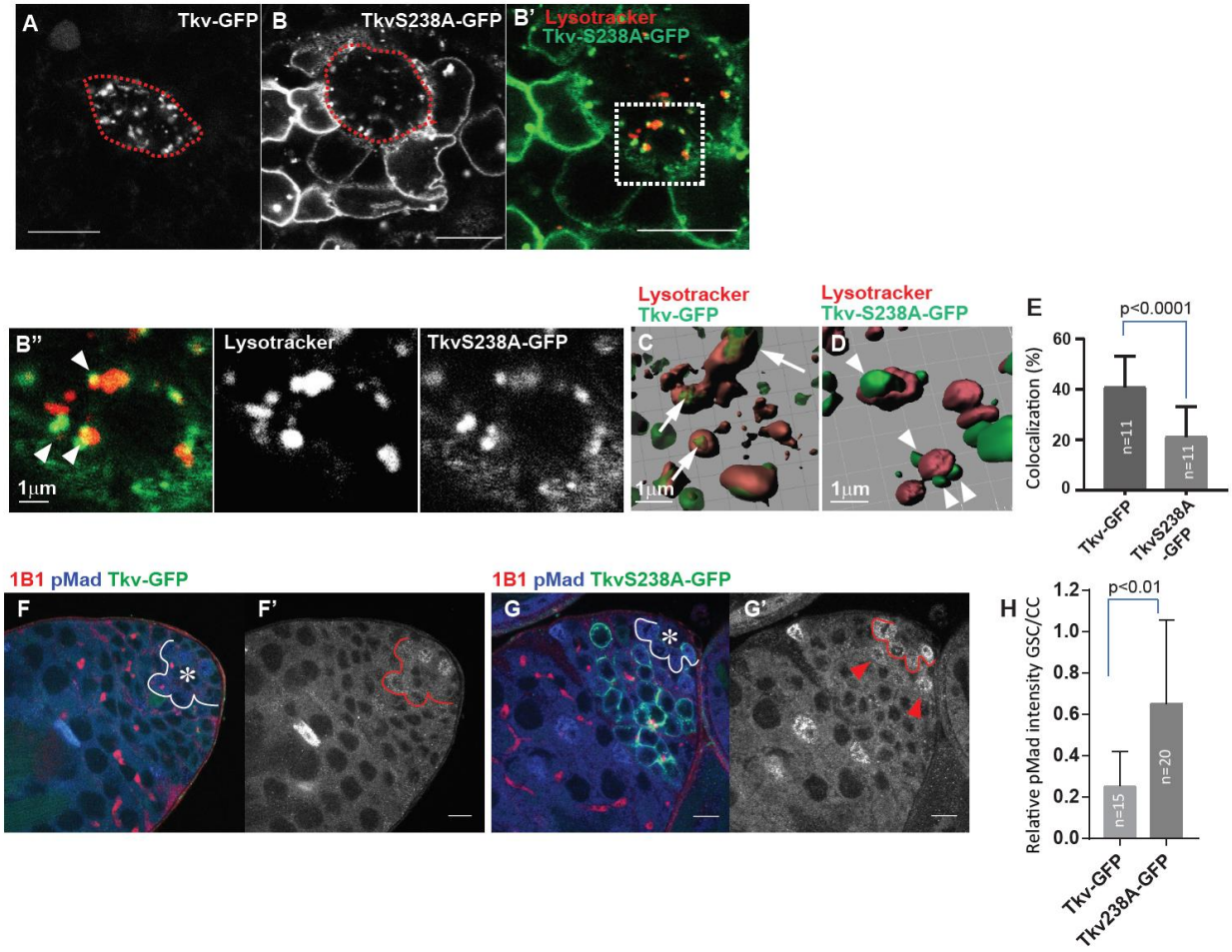
A
Tkv-GFP
B
TkvS238A-GFP
B'
Lysotracker
Tkv-S238A-GFP
B''
1μm
Lysotracker
TkvS238A-GFP
Lysotracker
Tkv-GFP
C
1μm
Lysotracker
Tkv-S238A-GFP
D
1μm
E
p<0.0001
Colocalization (%)
60
40
20
0
n=11
n=11
Tkv-GFP
TkvS238A-GFP
1B1 pMad Tkv-GFP
F
F'
1B1 pMad TkvS238A-GFP
G
G'
H
p<0.01
Relative pMad intensity GSC/CC
1.2
1.0
0.8
0.6
0.4
0.2
0.0
n=15
n=20
Tkv-GFP
Tkv238A-GFP

Figure 4

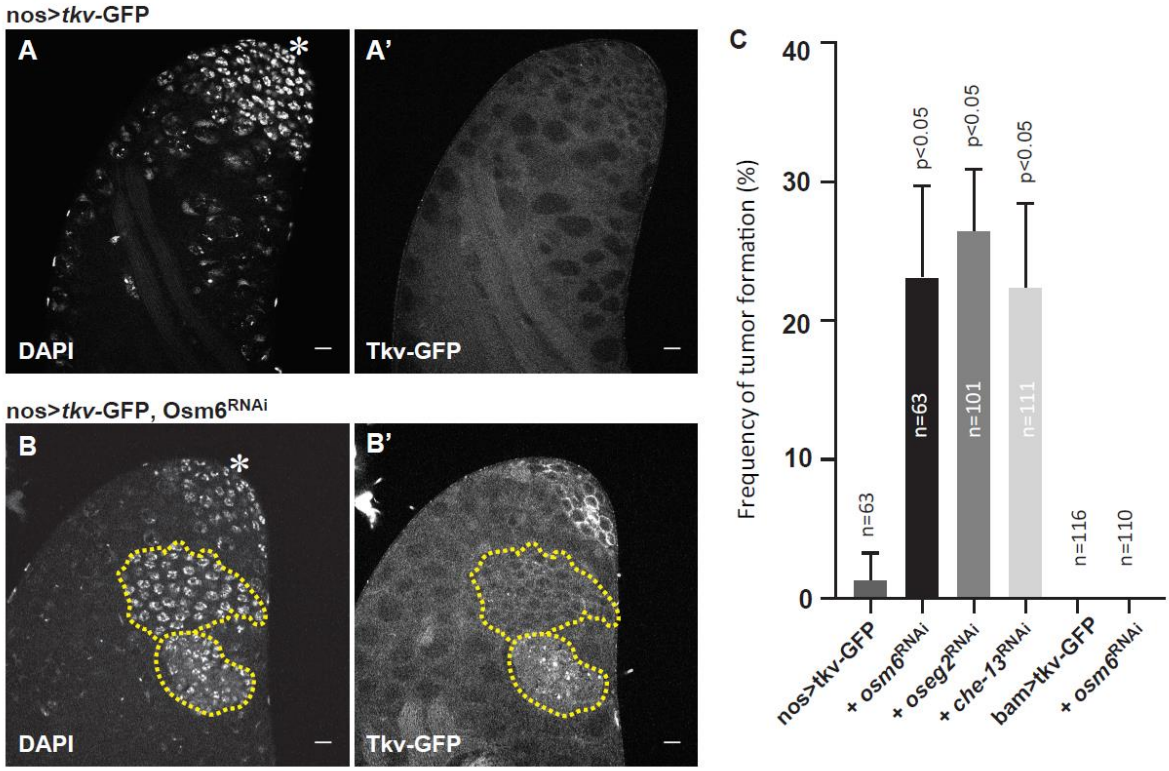
nos>tkv-GFP
A
A'
DAPI
Tkv-GFP
nos>tkv-GFP, Osm6RNAi
B
B'
DAPI
Tkv-GFP
C
Frequency of tumor formation (%)
40
30
20
10
0
p<0.05
p<0.05
p<0.05
n=63
n=63
n=101
n=111
n=116
n=110
nos>tkv-GFP
+ osm6RNAi
+ oseg2RNAi
+ che-13RNAi
bam>tkv-GFP
+ osm6RNAi

Figure 5

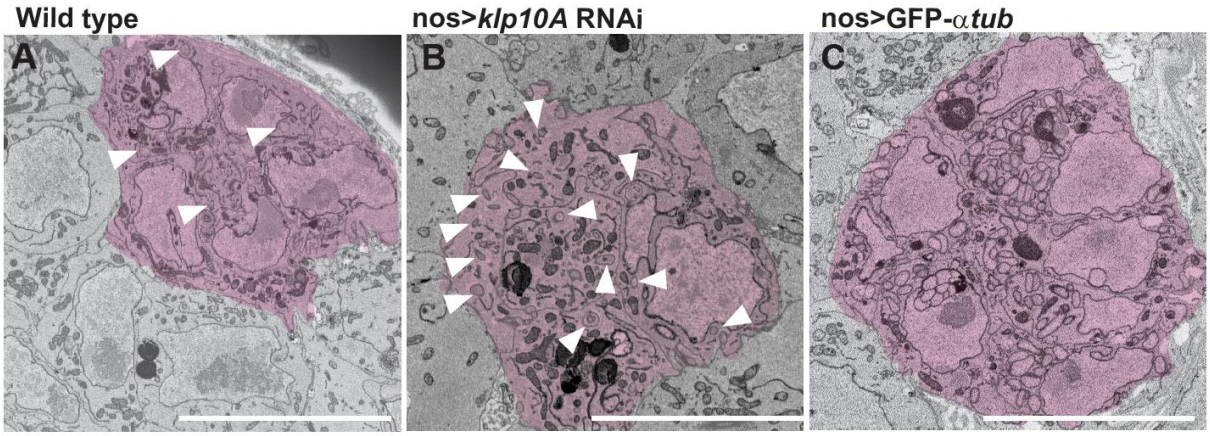

Methods

Fly husbandry and strains. All fly stocks were raised on standard Bloomington medium at 25°C (unless temperature control was required), and young flies (0- to 4-day-old adults) were used for all experiments. The following fly stocks were used: tkv-venus protein trap line (CPTI-002487) was a gift from B. McCabe. hs-flp; nos-FRTstop-FRT-gal4, UAS–GFP[25] ; nosGal4[26], updGal4 (FBti0002638) and UAS-dome-EGFP [27] were gift from Y. Yamashita. tubGal80^{ts} [28] (Gift from C.Y. Lee), bamGal4VP16 (gift from M. Buszczak), UAS-Dpp-mCherry [29] , UAS-Tkv-mCherry [29], UAS-Tkv-GFP [29] (gift from T. Kornberg and S. Roy), Oseg2 RNAi (Vienna Drosophila Resource Center, VDRC GD8122), Osm6 RNAi (VDRC GD24068). Other stocks were from Bloomington Stock Center, UAS–GFP–αTubulin (BDSC7253 or BDSC7373); Spin RNAi (TRiP.JF02782), Lamp1 RNAi (TRiP.HMS01802), Dor RNAi (TRiP.HMS03720), Shrb RNAi (TRiP.HMS01767). For the updGal4^{ts} driver, combination of updGal4 and tubGal80^{ts} [28] was used. Temperature shift crosses were performed by culturing flies at 18°C to avoid lethality during development and shifted to 29°C upon eclosion for 5days before analysis.
Control crosses for RNAi screening were designed with matching gal4 and UAS copy number using TRiP background stocks (BDSC36304 or BDSC35787) at 25 ℃. RNAi screening of candidate genes for Tkv trafficking and degradation was performed by driving UAS-RNAi constructs under the control of nosGal4 or updGal4 (see below for validation method).

Generation of Tkv S238A transgenic flies. EGFP cDNA were amplified from Drosophila gateway pPGW vector (https://emb.carnegiescience.edu/drosophila-gateway-vector-collection#_Copyright,_Carnegie) using following primers with restriction sites (underlined).
BglII GFP F 5'- AC<u>AGATCT</u>ATGGTGAGCAAGGGCGAGGAGCTGTTCA-3'
AscI GFP R 5'-TA<u>GGCGCGCC</u>TTACTTGTACAGCTCGTCCATGCCGAGA-3'
then digested with BglII and AscI. NotI BglII sites (underlined) were attached to gBlock TkvS238A fragment (Integrated DNA Technologies, sequence as follows).
5'-
AT<u>GCGGCCGC</u>ACCATGGCGCCGAAATCCAGAAAGAAGAAGGCTCATGCCCGCTCCCTAACC
TGCTACTGCGATGGCAGTTGTCCGGACAATGTAAGCAATGGAACCTGCGAGACCAGACCCG
GTGGCAGTTGCTTCAGCGCAGTCCAACAGCTTTACGATGAGACGACCGGGATGTACGAGGA
GGAGCGTACATATGGATGCATGCCTCCCGAAGACAACGGTGGTTTTCTCATGTGCAAGGTAG

CCGCTGTACCCCACCTGCATGGCAAGAACATTGTCTGCTGCGACAAGGAGGACTTCTGCAAC
CGTGACCTGTACCCCACCTACACACCCAAGCTGACCACACCAGCGCCGGATTTGCCCGTGAG
CAGCGAGTCCCTACACACGCTGGCCGTCTTTGGCTCCATCATCATCTCCCTGTCCGTGTTTAT
GCTGATCGTGGCTAGCTTATGTTTCACCTACAAGCGACGCGAGAAGCTGCGCAAGCAGCCAC
GTCTCATCAACTCAATGTGCAACTCACAGCTGTCGCCTTTGTCACAACTGGTGGAACAGAGT
TCGGGCGCCGGATCGGGATTACCATTGCTGGTGCAAAGAACCATTGCCAAGCAGATTCAGAT
GGTGCGACTGGTGGGCAAAGGACGATATGGCGAGGTCTGGCTGGCCAAATGGCGCGATGAG
CGGGTGGCCGTCAAGACCTTCTTTACGACCGAAGAGGCTTCTTGGTTCCGCGAGACTGAAAT
CTATCAGACAGTGCTGATGCGACACGACAATATCTTGGGCTTCATTGCCGCCGATATCAAGG
GTAATGGTAGCTGGACACAGATGTTGCTGATCACCGACTACCACGAGATGGGCAGCCTACA
CGATTACCTCTCAATGTCGGTGATCAATCCGCAGAAGCTGCAATTGCTGGCGTTTTCGCTGG
CCTCCGGATTGGCCCACCTGCACGACGAGATTTTCGGAACCCCTGGCAAACCAGCTATCGCT
CATCGCGATATCAAGAGCAAGAACATTTTGGTCAAGCGGAATGGGCAGTGCGCTATTGCTG
ACTTCGGGCTGGCAGTGAAGTACAACTCGGAACTGGATGTCATTCACATTGCACAGAATCCA
CGTGTCGGCACTCGACGCTACATGGCTCCAGAAGTATTGAGTCAGCAGCTGGATCCCAAGCA
GTTTGAAGAGTTCAAACGGGCTGATATGTATTCAGTGGGTCTCGTTCTGTGGGAGATGACCC
GTCGCTGCTACACACCCGTATCGGGCACCAAGACGACCACCTGCGAGGACTACGCCCTGCCC
TATCACGATGTGGTGCCCTCGGATCCCACGTTCGAGGACATGCACGCTGTTGTGTGCGTAAA
GGGTTTCCGGCCGCCGATACCATCACGCTGGCAGGAGGATGATGTACTCGCCACCGTATCCA
AGATCATGCAGGAGTGCTGGCACCCGAATCCCACCGTTCGGCTGACTGCCCTGCGCGTAAAG
AAGACGCTGGGGCGACTGGAAACAGACTGTCTAATCGATGTGCCCATTAAGATTGTCAGATC
TCA-3’

Synthesized fragments were annealed and digested by NotI and BglII. Resultant two inserts (TkvS238A and GFP) were ligated to modified pPGW vector using NotI and AscI sites in the multiple cloning site. Transgenic flies were generated using strain attP2 by PhiC31 integrase-mediated transgenesis (BestGene Inc.).

Immunofluorescent Staining. Immunofluorescent staining was performed as described previously[30]. Briefly, testes were dissected in phosphate-buffered saline (PBS) and fixed in 4% formaldehyde in PBS for 30–60 minutes. Next, testes were washed in PBST (PBS +0.3% TritonX-100) for at least 30 minutes, followed by incubation with primary antibody in 3% bovine serum albumin (BSA) in PBST at 4 °C overnight. Samples were washed for 60 minutes (three times for 20minutes each) in PBST, incubated with secondary antibody in 3% BSA in PBST at 4 °C overnight, and then washed for 60 minutes (three

times for 20 minutes each) in PBST. Samples were then mounted using VECTASHIELD with 4′,6-diamidino-2-phenylindole (DAPI) (Vector Lab, H-1200).
The primary antibodies used were as follows: 1B1 and rat anti Vasa (1:20), obtained from the Developmental Studies Hybridoma Bank (DSHB), Rabbit anti-Smad3 (phospho S423 + S425) antibody (1:100, Abcam, ab52903) AlexaFluor-conjugated secondary antibodies were used at a dilution of 1:400. Images were taken using a Zeiss LSM800 confocal microscope with a 63 ×oil immersion objective (NA=1.4) and processed using Image J and Adobe Photoshop software. Three-dimensional rendering was performed by Imaris software.

In situ hybridization

In situ hybridization on adult testes was performed mostly as described previously[31].
Briefly, testes were dissected in 1XPBS and then fixed in 4% formaldehyde/PBS for 45 min. After rinsed 2 times with 1XPBS, then resuspended in 70% EtOH, left overnight at 4°C. The next day, testes were washed briefly in the wash buffer containing 2XSSC and 10% deionized formamide, then incubated overnight at 37°C in the dark with the 50nM of Quasar® 570 labeled stellaris probe against dpp mRNA (LGC Biosearch Technologies, kind gift from Michael Buszczak) in the Hybridization Buffer containing 2XSSC, 10% Dextran sulfate (MilliporeSigma), 1μg/μl of yeast tRNA (MilliporeSigma), 2mM Vanadyl ribonucleoside complex (NEB), 0.02% RNAse free BSA (ThermoFisher) and 10% of deionized formamide. On the 3rd day, testes were washed 2 times for 30 min each at 37°C in the dark in the prewarmed wash buffer and then resuspended in a drop of VECTASHIELD with DAPI (Vector Lab, H-1200).

Chloroquine or Lysotracker/LysoSensor treatment

Testes from newly eclosed flies were dissected into Schneider's Drosophila medium containing 10% fetal bovine serum. Then testes were incubated at room temperature with or without 100μM Chloroquine in 1mL media for 4 hours prior to imaging. For the lysosome staining, testes were incubated with 50nM of LysoTracker Deep Red (ThermoFisher L12492) or 100nM of LysoSensor Green DND-189 (ThermoFisher L7535) probes in 1mL media for 10 min at room temperature then briefly rinsed with 1mL of media for 3 times prior to imaging. For Tkv-mCherry clonal expression, hs-flp; nos-FRTstop-FRT-gal4, UAS–GFP[25] with UAS-Tkv-mCherry, UAS-GFP-αTubulin flies were heat-shocked at 37°C. for 30 min. Testes were dissected 24 hour after heat shock.
These testes were placed onto Gold Seal™ Rite-On™ Micro Slides two etched rings with media, then covered with coverslips. An inverted Zeiss LSM800 confocal microscope with a 63 ×oil immersion objective (NA=1.4) was used for imaging.

Quantitative reverse transcription PCR to validate RNAi-mediated knockdown of genes. Males carrying nos-gal4 driver were crossed with males of indicated RNAi lines. Testes from 100-200 male progenies, age 0-7 days, were collected and homogenized by pipetting in TRIzol Reagent (ThermoFisher) and RNA was extracted following the manufacturer's instructions. 1μg of total RNA was reverse transcribed to cDNA using SuperScript III First-Strand Synthesis Super Mix (ThermoFisher) with Oligo (dT)20 Primer. Quantitative PCR was performed, in duplicate, using SYBR green Applied Biosystems Gene Expression Master Mix on an CFX96 Real-Time PCR Detection System (Bio-Rad). Control primer for
aTub84B (5'-TCAGACCTCGAAATCGTAGC-3'/5'-AGCAGTAGAGCTCCCAGCAG-3')
and experimental primer for
Spin (5'-GCGAATTTCCAACCGAAAGAG-3'/5'-CGGTTGGTAGGATTGCTTCT-3')
Shrb (5'-AGAGCGCCAACACAAACA-3'/5'-CACCTTGTCCACGTCCATATTC-3')
Dor (5'-CAGCGCAAGCAGCTTTATG -3'/5'-CGTCTCCTGGAATGTGTAGATG-3')
Lamp1 (5'-AACCATATCCGCAACCATCC-3'/5'-CCTCCCTAGCCTCATAGGTAAA-3')
were used. Relative quantification was performed using the comparative CT method (ABI manual). Only strains that showed less than 50% reduction of mRNA level were used (Lamp1 47.79%, Shrb 48.39%, Spin 25.05%, Dor 17.27%).

Quantification of Tkv-GFP positive GSC/testis.

Average intensity of Tkv-GFP in equator level of hub was used as the lower threshold for each testis. GSCs were judged as Tkv-GFP positive when the average intensity at the equator level of the cell was higher than set-threshold.

Quantification of pMad intensities.

For pMad quantification, integrated intensity within the GSC nuclear region was measured for anti-pMad staining and divided by the area. To normalize the staining condition, data were further normalized by the average intensities of pMad from randomly picked three cyst cells in the same testes, and the ratios of relative intensities were calculated as each GSC per average cyst cell.

Serial Block Face Scanning Electron Microscopy

Testes were dissected in PBS and fixed in 2.5% glutaraldehyde and 4% paraformaldehyde in a 0.1 M sodium cacodylate buffer. Samples were processed and imaged at Renovo Neural Inc. (Cleveland, USA) Samples were stained with heavy metals and embedded in Epon resin, and mounted onto pins (detailed

protocol available from Renovo Neural). Serial blockface images were obtained using a Zeiss Sigma VP scanning electron microscope equipped with a Gatan 3View in-chamber ultramicrotome.